S. Office of Naval Research.

NAVAL RESEARCH

REVIEWS

AUGUST 1976

407-c

Engin

The University of Michigan Engineering Library

THE UNIVERSITY OF MICHIGAN

OCT 19 1976

ENGINEERING LIBRARY

UNIVERSITY OF MICHIGAN LIBRARIES

OCT 7 1976

DEPOSITED BY THE UNITED STATES OF AMERICA

Digitized by Google

Original from UNIVERSITY OF MICHIGAN

Generated for member (University of Maryland, College Park) on 2014-10-01 20:07 GMT / http://hdl.handle.net/2027/mdp.39015000504624
Public Domain, Google-digitized / http://www.hathitrust.org/access_use#pd-google

PROFILES IN SCIENCE

Dr. Benjamin Lax

Dr. Benjamin Lax is Professor of Physics at M. I. T. and Director of the Francis Bitter National Magnet Laboratory. Previously he was in charge of the solid state program at the Lincoln Laboratory of which he was Associate Director. In 1960 Dr. Lax received the Oliver E. Buckley Prize for his pioneering work on cyclotron resonance and magneto-optical studies in semiconductors.

Since Dr. Lax has been at M. I. T., he has been active in quantum electronics, solid state, and plasma physics, involving high magnetic fields. Recent achievements under an ONR contract include noncolinear mixing of radiation from two CO_2 lasers to produce a tunable source at infrared and submillimeter wavelengths.

He is a member of the National Academy of Sciences and a Fellow of both the American Physical Society and the American Academy of Arts and Sciences.

Generated for member (University of Maryland, College Park) on 2014-10-01 20:07 GMT / http://hdl.handle.net/2027/mdp.39015000504624
Public Domain, Google-digitized / http://www.hathitrust.org/access_use#pd-google

Digitized by Google

Original from
UNIVERSITY OF MICHIGAN

Surface Effect Ship Sets World Speed Record

The U.S. Navy Surface Effect Ship SES-100B established a new Navy speed record today when it reached 103.03 miles per hour (89.4 knots) in St. Andrew's Bay off Panama City, Florida. The speed run marks a world record for surface type ships.

Aboard the SES-100B for this record setting run were Secretary of the Navy, J. William Middendorf II, and Captain Carl J. Boyd, USN, project manager for the Navy's surface effect ship project.

The 100B surface effect ship rides in the water on an air bubble contained by fixed sidewalls and flexible endseals. This configuration virtually eliminates wave drag so the SES is able to achieve high speed.

On April 8, 1976, while operating at 69 mph (60 knots), the SES-100B launched a standard missile. The launch was successful and the missile hit its target five miles away. This was the first missile to be launched from a surface effect ship, and also marked the first time any missile was launched vertically (perpendicular to the ocean surface) from a U.S. surface ship.

The SES-100B was built by Bell Aerospace Company, Division of Textron in 1971. The experimental craft has been undergoing testing and evaluation by the Navy at the Naval Coastal Systems Laboratory for the past two years. The ship has an overall length of 78 feet, a beam of 35 feet and a displacement of 100 tons. Propulsion is provided by three marine gas turbine engines.

The next SES to be built, a 3,000 ton prototype, will have open ocean capabilities. The larger SES will perform at speeds about three times as fast as conventional ships, and will operate with a crew of about 125 officers and enlisted men. Construction is scheduled to begin in FY 1978, for completion in 1981.

NAVAL RESEARCH REVIEWS publishes highlights of research conducted by Navy laboratories and contractors and describes important naval experimental facilities. Manuscripts submitted for publication, correspondence concerning prospective articles, and changes of address, should be directed to Code 730, Office of Naval Research, Arlington, Va. 22217. Requests for subscriptions should be directed to the Superintendent of Documents, U.S. Government Printing Office, Washington, D.C., 20402. Subscription price: $6.50 per year in the U.S. and Canada; $8.15 per year, foreign; $0.55 per individual copy. The issuance of this periodical approved in accordance with Dept. of the Navy publications and printing regulations.

Editor: WILLIAM J. LESCURE

NAVSO P-510

Associate Editors:

A. R. LAUFER, ONR PASADENA
A. R. DAWE, ONR CHICAGO
A. L. POWELL, ONR BOSTON
D. A PATTERSON, NAVAL RESEARCH LABORATORY

Generated for member (University of Maryland, College Park) on 2014-10-01 20:07 GMT / http://hdl.handle.net/2027/mdp.39015000504624
Public Domain, Google-digitized / http://www.hathitrust.org/access_use#pd-google

Digitized by Google

Original from
UNIVERSITY OF MICHIGAN

MESSAGE FROM THE ASSISTANT SECRETARY OF THE NAVY FOR RESEARCH AND DEVELOPMENT

This year the Office of Naval Research celebrates its 30th Anniversary. The event is a milestone in a long tradition of collaboration between the Navy and the scientific community of the United States – a collaboration that began well before what we call modern science appeared on the scene. In 1885, Secretary of the Navy William C. Whitney stated in his annual report, "It is of little service to a nation to have any Navy at all unless it is a fair expression of the highest scientific resources of its day."

Public Law 588, signed by President Truman on August 1, 1946, created the Office of Naval Research in the Office of the Secretary of the Navy and charged it, among other things, with the duty to encourage and promote naval research and to conduct naval research in augmentation of work proceeding elsewhere in the Navy.

In fulfillment of those duties, the Office of Naval Research has made an outstanding contribution not only to the Navy, but to the whole nation through its contract research program. Through this program, ONR was able, from its beginning, to attract distinguished members of the civilian scientific community to a program of basic research aimed at providing the base for future technology and its optimum utilization by the Navy. This was done by providing for their research equipment and helping with the salaries of their assistants. But of more and lasting importance, ONR evolved policies and procedures which pointed the way to increase the participation of the Federal Government in a comprehensive program of scientific research throughout the country.

In parallel with the contract program, the Office of Naval Research has encouraged basic research in the civil service laboratories of the Navy. The Naval Research Laboratory, which reports directly to the Chief of Naval Research, is known throughout the world as one of the finest basic research laboratories of the Federal government. In its role as the corporate research laboratory of the Navy, NRL is the focal point for the Navy's in-house research and serves as a highly successful intermediary among the fleet, the other laboratories, industry, and the world of academic science. Its program is marked by a high degree of initiative, in the best scientific tradition, and ranges over most of the spectrum of research interests in the Navy, from the space sciences to the protection of underwater structures from environmental degradation.

I want to emphasize that the Office of Naval Research plays a creative and important role between the researcher, whether in a government laboratory or in the private community, and the long-term needs of the Navy. ONR supports university research and government research with the spirit that makes sense to those organizations. Deliberately, it has not compromised the motives of the individual research workers and their organizations. At the same time, the Office successfully shapes an overall program of research which contributes to solutions of the Navy's long-term problems.

Digitized by Google
Original from
UNIVERSITY OF MICHIGAN
Generated for member (University of Maryland, College Park) on 2014-10-01 20:07 GMT / http://hdl.handle.net/2027/mdp.39015000504624
Public Domain, Google-digitized / http://www.hathitrust.org/access_use#pd-google

Thirty years ago ONR had the distinction of being the sole source of government support for basic research in our universities and in the Navy. Under these circumstances ONR earned and still holds the respect, I might say affection of the scientific community. Only by preserving within ONR an atmosphere attractive to the new generation of creative scientists for whose services the competition becomes keener every day, can the Navy bring to bear upon its problems the best minds of the future. I am confident that the next 30 years of ONR will demonstrate that the Navy has met this challenge.

H. TYLER MARCY
Assistant Secretary of the Navy
(Research and Development)

Generated for member (University of Maryland, College Park) on 2014-10-01 20:07 GMT / http://hdl.handle.net/2027/mdp.39015000504624
Public Domain, Google-digitized / http://www.hathitrust.org/access_use#pd-google
Digitized by Google
Original from
UNIVERSITY OF MICHIGAN

MESSAGE FROM THE CHIEF OF NAVAL RESEARCH

1976 marks the 30th Anniversary of the Office of Naval Research. This makes me keenly aware of the honor and responsibility I have in continuing the proud tradition of my office.

Since its inception, ONR has represented the Navy in Science, coordinated naval scientific research, maintained liaison with the scientific community both in this country and abroad, and cooperated with other government agencies in furthering basic research. It has supported scientific research in nearly every major scientific field and its research results have made our Navy second to none. Countless significant benefits have also accrued to the civilian economy.

ONR will continue to be deeply involved in science in order to keep abreast of scientific progress and ahead of our potential adversaries. A hundred years ago when science was a casual, slow moving effort, the Navy could afford to wait for a new piece of hardware until an inventor had worked it out. Today, however, scientific research is a broad, organized, expensive, fast moving effort. No longer can the Navy afford to be a mere spectator, standing by to purchase items, if they appear useful. The Navy must actually be in science. It must conduct its own research and support the work of others. Thus, the Office of Naval Research will continue its support of basic research to meet future emergencies that will require the nation to be self-sufficient in all fields of science.

Our objective during the 30th Anniversary Year is to review the current status and future of science from a perspective of past accomplishments. Our challenge is to identify the scientific opportunities of today, to evaluate these in terms of the future needs of the Navy, and to assure ourselves that we are responding to these needs and opportunities with the same vision, dedication, and courage as did our predecessors.

R. K. GEIGER
Rear Admiral, USN

Generated for member (University of Maryland, College Park) on 2014-10-01 20:07 GMT / http://hdl.handle.net/2027/mdp.39015000504624
Public Domain, Google-digitized / http://www.hathitrust.org/access_use#pd-google
Digitized by Google
Original from UNIVERSITY OF MICHIGAN

Sunlight and the Ocean

Gilbert N. Plass and George W. Kattawar*
Texas A and M University

The long-range scientific objective of the research described here is to obtain a better understanding of the radiance and polarization of the light distributed within the ocean and reflected by it back into the atmosphere. The Office of Naval Research is supporting this work so that the Navy will have a better understanding of the radiation present in the oceans. The possibility of viewing and discriminating objects underwater depends critically on the background illumination. A better understanding of background illumination and its polarization will come from this study. The influence of the light intensity and polarization on marine animals is a subject of recent interest to the Navy, particularly since polarized light has been found to produce important behavioral reaction in some aquatic life forms. Another important area of interest is the photosynthetic activity in the sea. The chlorophyll content of the phytoplankton affects the polarization of light traveling in sea water. Techniques for the detection of surface contaminants either from aircraft or surface vessels by polarization sensing devices could result from this work. Studying the effect of wind velocity on the distribution of the radiation field both below and above the ocean may lead to methods for determining various oceanic parameters from satellites such as the sea state, phytoplankton concentration, and the amount of hydrosols in the ocean.

Photons in the Atmosphere

The brightness and color of the ocean when seen by natural sunlight is determined by the interaction of the sunlight with the atmosphere, the ocean surface, and the various substances in the ocean. As any substance in any of these regions changes, there are corresponding changes in the reflected and transmitted light which can tell us a great deal about the state of the ocean and atmosphere.

The path of a solar photon after it enters the earth's atmosphere can be exceedingly complex. The photon may be absorbed by

*Dr. Plass is Head of the Physics Department at Texas A and M University. Dr. Plass and Dr. Kattawar, who are both Professors of Physics at Texas A and M do research in the field of atmospheric and planetary physics specializing in radiative transfer in the earth's atmosphere.

Generated for member (University of Maryland, College Park) on 2014-10-01 20:07 GMT / http://hdl.handle.net/2027/mdp.39015000504624
Public Domain, Google-digitized / http://www.hathitrust.org/access_use#pd-google
Digitized by Google
Original from UNIVERSITY OF MICHIGAN

various molecules such as ozone and water in the atmosphere. This absorption varies with wavelength and is particularly strong at some ultraviolet wavelengths for ozone and at some infrared wavelengths for water molecules. The photon may be scattered by any of the molecules in the atmosphere and also by density fluctuations in the gaseous medium. This is called Rayleigh scattering; its most important characteristic is that the scattering is proportional to the inverse fourth power of the wavelength. Thus the blue light is scattered much more than the red, because of its shorter wavelength. When we look at the blue sky we are observing photons that have been scattered one or more times out of the direct solar beam, mainly by Rayleigh scattering.

Usually the sky on a clear day is a deep blue near the zenith and a much lighter color near the horizon. Obviously factors other than Rayleigh scattering influence the color. The small particles suspended in the atmosphere are called aerosols. They include natural substances such as plant oils, sea spray, and particles of rock blown into the atmosphere, as well as man-made pollutants such as carbon particles and all the other substances released into the atmosphere by industrial processes. Many of these particles have sizes greater than one micrometer and thus are larger than the typical wavelength of visible light. The aerosol distributions scatter and absorb the light, but usually in a very different manner than happens for Rayleigh scattering. Both theory and experiment show that the scattering has only a small dependence on wavelength in the visible spectrum, unlike the strong wavelength dependence of Rayleigh scattering. Thus, light scattered by aerosols is nearly white, since all wavelengths are scattered equally (to a first approximation). The white on the horizon on a typical day is caused by the light scattered from the aerosols. It is more prominent on the horizon, because the light observed in that direction passes through a longer atmospheric path near the earth's surface.

There is a second important difference in the scattering of light by aerosols compared to Rayleigh scattering. In the latter case the amount of scattered light depends only slightly on the angle through which the photon is scattered. On the other hand when a photon is scattered by an aerosol somewhat larger than the wavelength of light, the majority of the photons are scattered through a relatively small angular range around the original direction. This effect has important consequences for the penetration of light in various media including the ocean where the hydrosols (various organic and inorganic particles in the water) scatter the light in a manner similar to the aerosols.

Digitized by Google

Original from
UNIVERSITY OF MICHIGAN

Generated for member (University of Maryland, College Park) on 2014-10-01 20:07 GMT / http://hdl.handle.net/2027/mdp.39015000504624
Public Domain, Google-digitized / http://www.hathitrust.org/access_use#pd-google

Liquid water drops are also important in the atmosphere. When they exist in sufficient density, they are observed as clouds which take many different forms. There are the white isolated cumulus clouds—white because the water droplets have sizes ranging from one to several hundred microns; thus there is little wavelength dependence in the scattering. When the sky is completely overcast with clouds, it appears grey to our eye. This is really just a white of a lower intensity. The photons that manage to get through a thick overcast have undergone multiple scatterings within the cloud before some of them finally emerge from the lower boundary of the cloud. There is little wavelength dependence in the visible to either the scattering or absorption processes within the cloud.

Photons on the Ocean Surface

When a photon reaches the ocean surface, it may either be reflected from the surface or refracted as it enters the ocean. Only 2% of the photons are reflected when they strike the surface from the zenith direction. The fraction reflected at other incident directions increases as the zenith angle increases, until all of the light is reflected at grazing incidence. The fraction reflected also depends on the polarization of the light. A light beam may be resolved into two components whose electric vectors vibrate at right angles to each other in the plane perpendicular to the direction of propagation. When the amplitude of these two vectors is the same, and there is no definite phase relationship between them the light is said to be unpolarized; otherwise it is polarized. The most striking demonstration of this is when the incident light has a zenith angle of 53° (Brewster's angle); in this case, the reflected light is completely plane polarized with the electric vector perpendicular to the principal plane containing the incident and zenith directions.

The light that enters the ocean from the atmosphere is refracted toward the zenith according to Snell's law. When the upwelling light within the ocean reaches the surface, it also is either reflected back into the ocean or refracted as it passes into the atmosphere. In this case the refraction bends the light ray away from the zenith direction and has the consequence that, if the ray has a zenith angle of 48° within the ocean, it is refracted so that it has a nearly horizontal direction in the atmosphere. Rays from below incident on the surface at zenith angles greater than 48° can not enter the atmosphere and are instead totally internally reflected. Again there are interesting polarization effects, as the downwelling light just

Digitized by Google
Original from UNIVERSITY OF MICHIGAN
Generated for member (University of Maryland, College Park) on 2014-10-01 20:07 GMT / http://hdl.handle.net/2027/mdp.39015000504624
Public Domain, Google-digitized / http://www.hathitrust.org/access_use#pd-google

below the surface that has undergone total internal reflection has a relatively high degree of elliptical polarization (the resultant electric vector of the light beam moves in an elliptical path) (Figure 1).

Within the ocean the photons are absorbed and scattered by the water molecules and density fluctuations as well as by the hydrosols . Water is most transparent in the blue-green portion of the spectrum. The absorption becomes much larger toward the red end of the spectrum as well as in the ultraviolet and infrared regions. The hydrosols have various size distributions depending on their nature, but the particles are usually in the 0.1 to 10 micrometer size range and preferentially scatter the light in the forward direction.

The real ocean surface has waves, which introduce another complexity into the theory. Fortunately the distribution of wave slopes is known fairly well from measurements made for various surface wind velocities. Perhaps the easiest phenomenon to simulate involving light and the ocean is the bright glitter pattern observed on the surface when looking down on the ocean in certain directions. Individual flashes of light are observed when a wave slope within the angle of observation has just the right inclination to reflect the sun's rays at the mirror angle to the observer. If the ocean surface were completely calm, a perfect mirror image of the sun would be observed reflected from the surface at the appropriate angle. As the wind and waves increase in intensity, this image is spread out over a wider and wider area (Figure 2).

The time averaged intensity of the glitter pattern can be calculated from a knowledge of the probability of occurrence of various wave slopes. From this theory the changes in the glitter pattern with wind

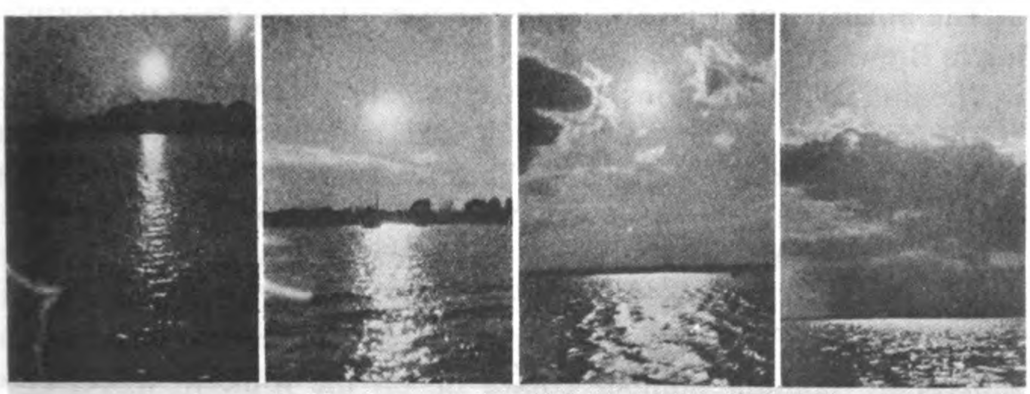

a b c d

Figure 1 — Reflection of sun on ocean for solar elevation angles of 7°, 13°, 20°, and 30° and breeze of 3, 10, 18 knots respectively for a, b, c, and d. (From E. O. Hulbert, J. Opt. Soc. Amer. **24***, 35 (1934)).*

217-363 O - 76 - 2

Digitized by Google

Original from UNIVERSITY OF MICHIGAN

Generated for member (University of Maryland, College Park) on 2014-10-01 20:07 GMT / http://hdl.handle.net/2027/mdp.39015000504624
Public Domain, Google-digitized / http://www.hathitrust.org/access_use#pd-google

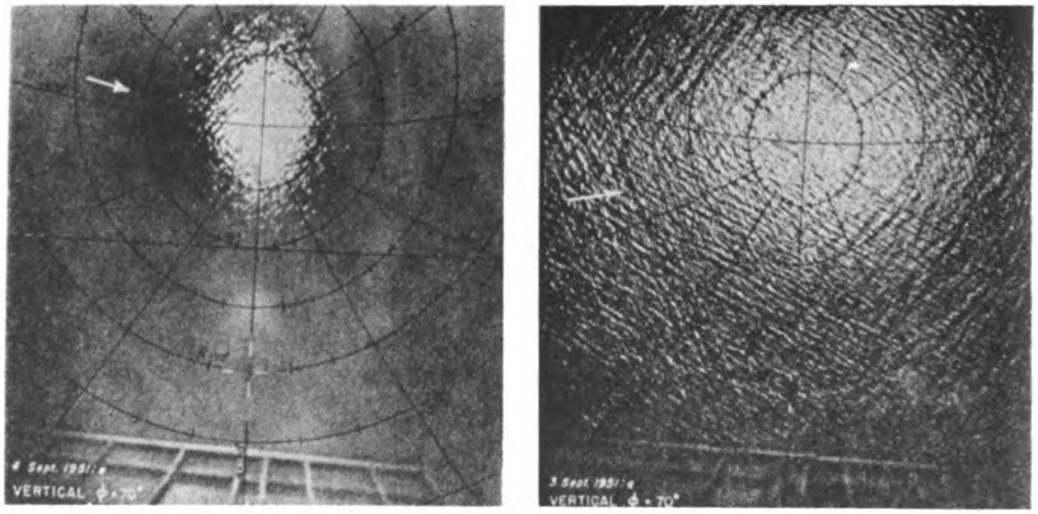

Figure 2 — Glitter patterns photographed by an aerial camera pointing vertically downward for a solar zenith angle of 20°. There were larger wave slopes on the right. (From C. Cox and W. Munk, J. Opt. Soc. Amer. **44***, 838 (1954)).*

velocity and the sun's zenith angle can be studied. In general the pattern broadens as the wind speed increases and elongates as the sun approaches the horizon. The maximum radiance is near the mirror angle when the waves are small; the case when the wind speed is 0.5 m/sec is shown in Figure 3 for a solar zenith angle of 30°. The maximum intensity is near the mirror angle (zenith angle, $\theta_y = 30°$). However, when the wind speed has increased to 15 m/sec, the maximum intensity is at 43° (Figure 4). A great deal of information can be obtained about the wave slopes from observations of the glitter pattern made from airplanes or satellites. The radiation in the glitter pattern is strongly polarized at many angles as shown in Figure 5. The polarization is nearly 100% at angles of reflection corresponding to Brewster's angle.

Theoretical calculations of the complete radiation field in the atmosphere and ocean are difficult and complex. A Monte Carlo technique is the only one that has been used successfully to solve this problem up to the present time, although we are working on a matrix operator method also. The Monte Carlo method has this picturesque name because random numbers are used to choose a particular event from among a large number of possible outcomes, much as a supposedly random number comes up on the roulette wheel at a gaming table. For example, if the probability of scattering a photon for each possible range of scattering angles is known, a random number can be used in connection with this probability distribution to select a particular scattering angle. If this process is repeated a

Digitized by Google
Original from
UNIVERSITY OF MICHIGAN
Generated for member (University of Maryland, College Park) on 2014-10-01 20:07 GMT / http://hdl.handle.net/2027/mdp.39015000504624
Public Domain, Google-digitized / http://www.hathitrust.org/access_use#pd-google

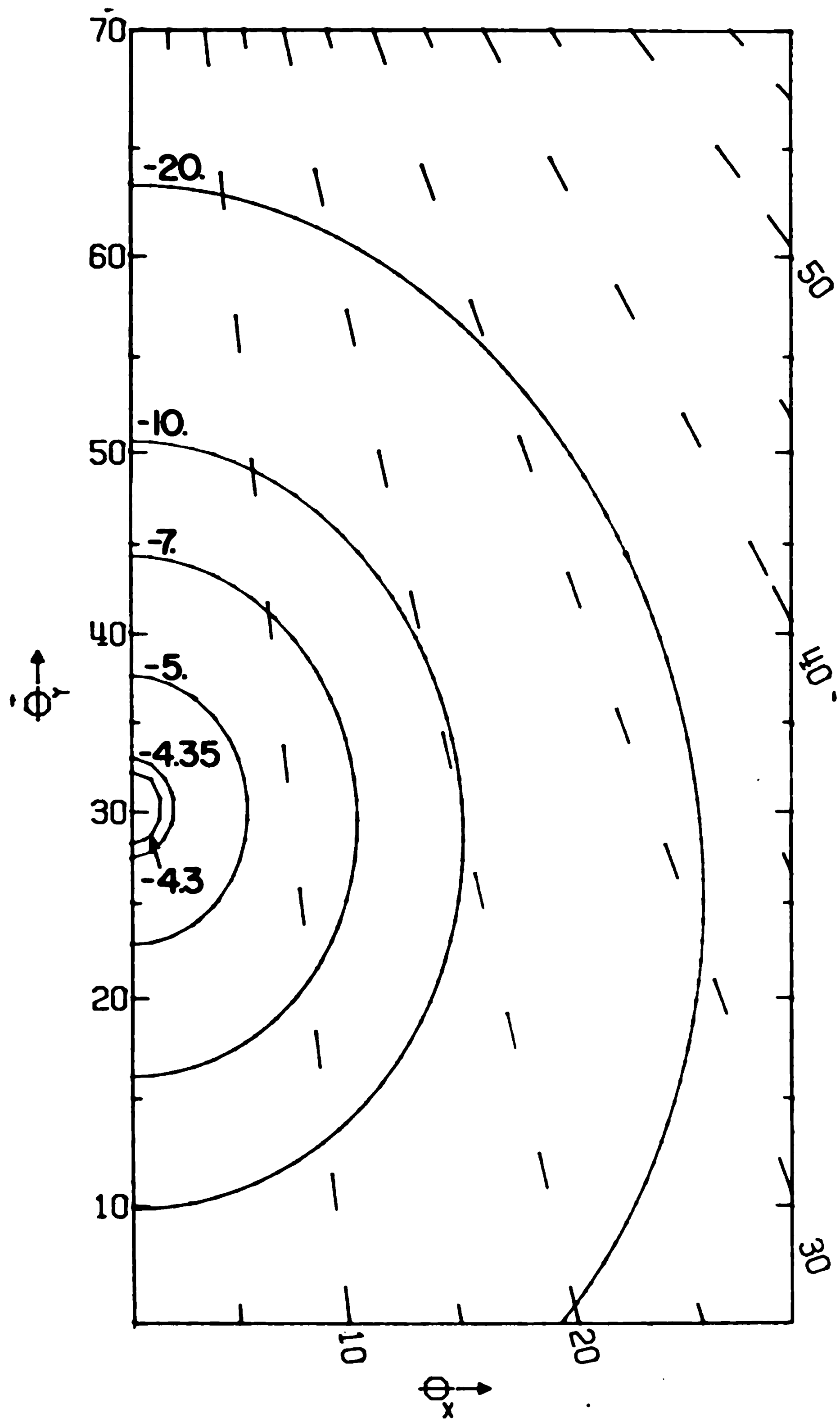

Figure 3 – Time averaged intensity of glitter pattern as it would be observed by a camera pointed at a zenith angle of 30°. The solar zenith angle is 30° and the wind speed is 0.5 m/s. The curved lines connect points of equal intensities; the logarithm to base 10 of the intensity is marked on the curves.

Generated for member (University of Maryland, College Park) on 2014-10-01 20:07 GMT / http://hdl.handle.net/2027/mdp.39015000504624
Public Domain, Google-digitized / http://www.hathitrust.org/access_use#pd-google
Digitized by Google
Original from UNIVERSITY OF MICHIGAN

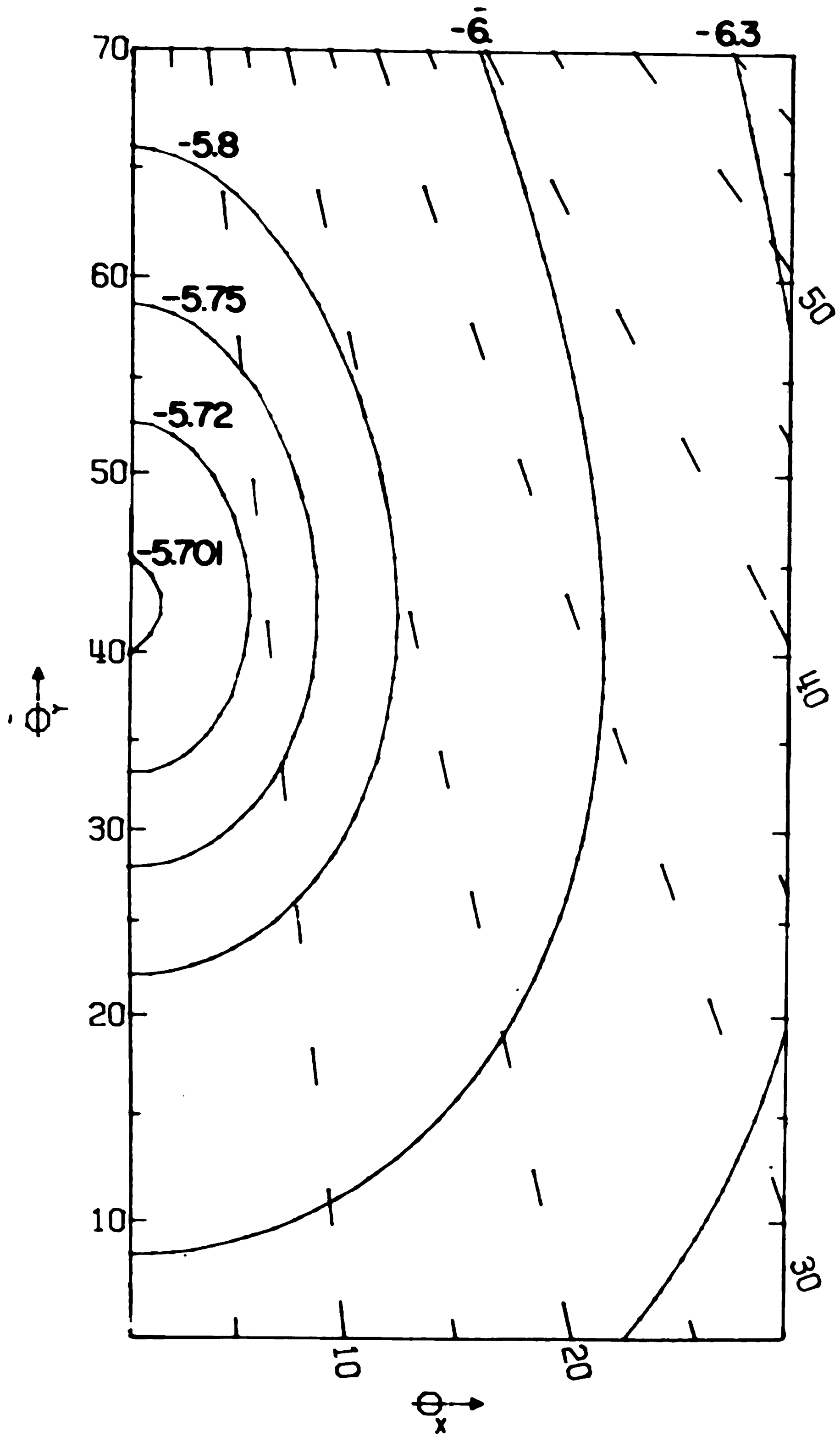

Figure 4 — Same as Figure 3 except windspeed is 15 m/s.

Generated for member (University of Maryland, College Park) on 2014-10-01 20:07 GMT / http://hdl.handle.net/2027/mdp.39015000504624
Public Domain, Google-digitized / http://www.hathitrust.org/access_use#pd-google
Digitized by Google
Original from
UNIVERSITY OF MICHIGAN

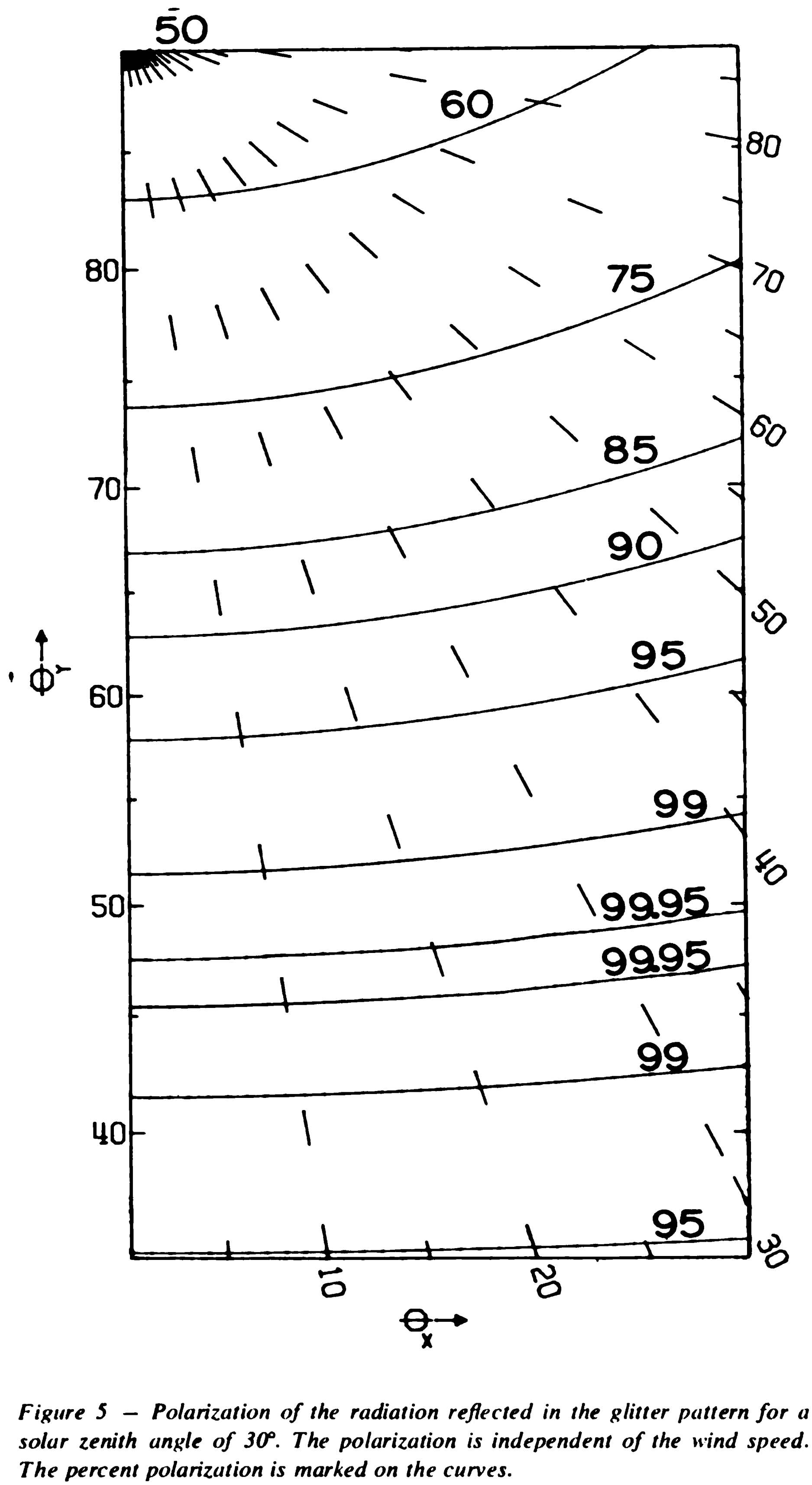

Figure 5 — Polarization of the radiation reflected in the glitter pattern for a solar zenith angle of 30°. The polarization is independent of the wind speed. The percent polarization is marked on the curves.

217-363 O - 76 - 3

Digitized by Google
Original from UNIVERSITY OF MICHIGAN
Generated for member (University of Maryland, College Park) on 2014-10-01 20:07 GMT / http://hdl.handle.net/2027/mdp.39015000504624
Public Domain, Google-digitized / http://www.hathitrust.org/access_use#pd-google

large number of times, the number of photons scattered into each infinitesimal range of angle closely reproduces the original distribution function.

In the Monte Carlo method a solar photon enters the atmosphere at an angle corresponding to the solar zenith angle. First, the height at which the first interaction with an atmospheric particle occurs is chosen by a random number from a knowledge of the total cross section as a function of height. Since the probability of absorption is known, another random number determines whether the photon is scattered or absorbed (the actual calculations are more sophisticated, as will be described shortly). If the photon is scattered, a third random number is used together with the scattering distribution to determine the angle at which the photon is scattered. The photon continues on its way and may make any required number of such collisions until it finally arrives at the ocean surface. Of course many photons arrive at the surface without making any atmospheric collisions and comprise the direct solar beam. On the other hand, those that have made one or more collisions represent the radiation from the blue sky. At the ocean surface the probability of reflection is known as a function of the angle of incidence. Thus, another random number decides whether the photon is reflected or transmitted at the surface. If waves are present, still another random number is used to select a particular wave slope from the appropriate distribution function. If the photon is reflected from the ocean surface, it continues on its path initially traveling upward in the atmosphere and may make more collisions there, in which case it may even be scattered downward to reach the ocean surface a second time.

If the photon enters the ocean surface, a new direction of travel is computed from Snell's law of refraction. The position of the first collision in the ocean is determined from the total cross section in the ocean. A random number is used to determine whether the photon is absorbed by a water molecule or one of the hydrosols. If it is scattered, the scattering angle is chosen from the appropriate distribution function for scattering from hydrosols in ocean water. The photon may eventually be traveling in an upward direction and reach the under side of the ocean surface. Again it may be reflected or transmitted. If the incident zenith angle is greater than the critical angle, only total internal reflection is allowed. Detectors may be placed at any location in the atmosphere or ocean in the calculation to record the number of photons that arrive from any specified range of solid angle.

Digitized by Google
Original from
UNIVERSITY OF MICHIGAN
Generated for member (University of Maryland, College Park) on 2014-10-01 20:07 GMT / http://hdl.handle.net/2027/mdp.39015000504624
Public Domain, Google-digitized / http://www.hathitrust.org/access_use#pd-google

The calculation of photon paths in the manner described above can be done very efficiently on a large computer. A large number of photons are used in order to obtain good statistics in the final results. A typical run that includes the effects of ocean waves takes about 10 min. on a CDC 7600 during which time almost 2,000,000 photon collisions are calculated.

There are actually a number of refinements in the simple scheme described above that greatly improve the statistical accuracy of the results for a given amount of computing time. One of the most important of these is the concept of statistical weights. Each photon is assigned such a weight which is initially unity. No photon path is terminated because of absorption, but instead the weight is appropriately adjusted. For example, if the probability of absorption for a particular collision is 0.8, the weight is multiplied by 0.2, the fraction of photons that survive this particular collision, and the photon is then scattered at an appropriate angle. Similarly no photons are lost out of the top of the atmosphere; instead a collision is always forced for a photon traveling upward, and the weight is appropriately adjusted. In this scheme no photon is ever lost by absorption or by leaving the top of the atmosphere; the calculation is terminated only when the weight falls below a predetermined number, usually taken as 10^{-6}.

A few results of these calculations are shown here. When the sun is directly overhead at the zenith, the radiance just above the ocean surface, as well as just below, is shown in Figure 6. The radiance is plotted as a function of the zenith angle of observation. All of these results are for the principal plane defined as the plane that contains the solar direction and the zenith. The radiation coming downward from the zenith is at the left of the figure, the radiation from the horizon is at the center, and the upward radiation from the nadir is at the right. A smooth ocean is assumed here. The upwelling radiation observed just above the ocean surface falls off rapidly from the horizon, since the fraction of sky radiation reflected also decreases rapidly as the zenith angle of the reflected radiation decreases from 90°. The peak in the upwelling radiation at the nadir is from the reflection of the solar beam.

Just beneath the ocean surface the downwelling radiation is relatively strong from the zenith to the critical angle of 48°. It then falls in intensity by an order of magnitude, since no light can enter a calm ocean from outside this allowed cone. The entire intensity outside of the allowed cone arises from upwelling photons that are totally internally reflected at the ocean surface into the downward direction.

Digitized by Google
Original from
UNIVERSITY OF MICHIGAN
Generated for member (University of Maryland, College Park) on 2014-10-01 20:07 GMT / http://hdl.handle.net/2027/mdp.39015000504624
Public Domain, Google-digitized / http://www.hathitrust.org/access_use#pd-google

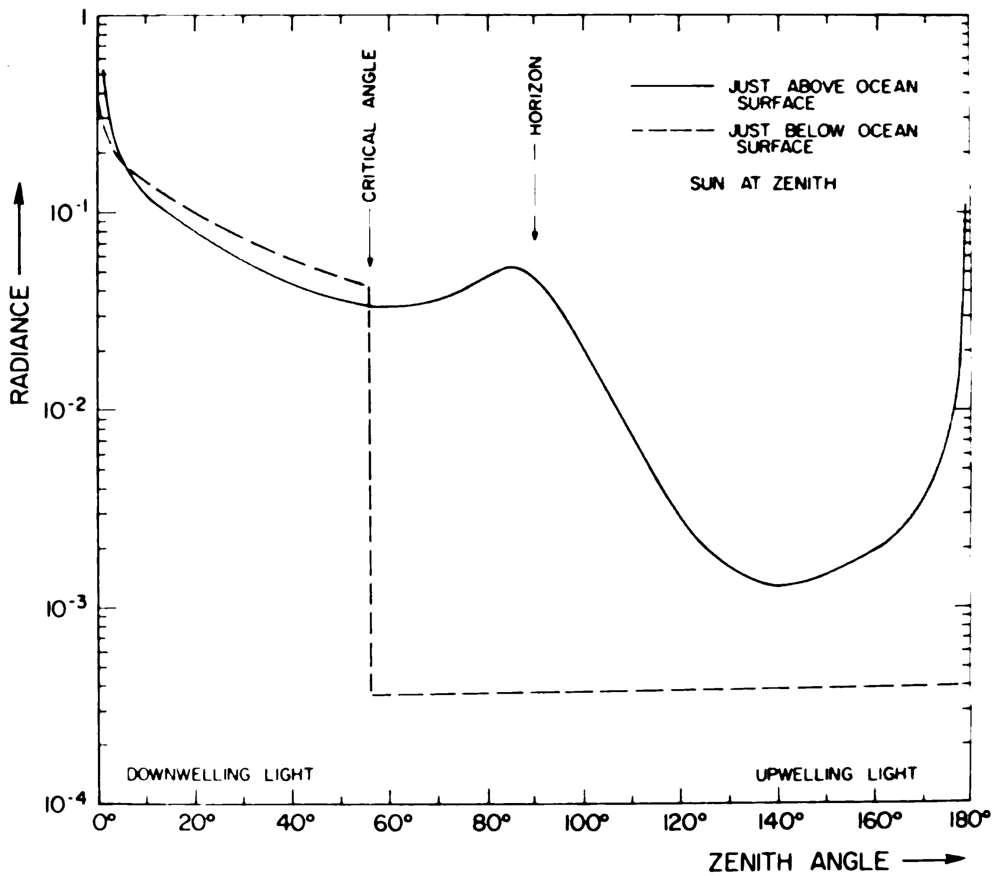

Figure 6 – The radiance just above and just below the ocean surface as a function of the zenith angle of observation when the sun is at the zenith.

The same general features occur at other solar zenith angles. The radiance for a solar zenith angle of 81.4° is shown in Figure 7. Within the ocean the direct solar beam is observed nearer the zenith than in the atmosphere, at an angle determined by the law of refraction (47.6° in this case). When the sun is near the horizon, the downwelling radiation in the ocean within the allowed cone is often several orders of magnitude greater than outside of it.

Polarization effects have been included in the Monte Carlo calculations by a calculation of what is known as the Stokes vector. When the four components of this vector are calculated, it is possible to obtain both the polarization and ellipticity of the radiation. An example of this is shown in Figure 8 with the sun at the zenith. Just above the ocean surface the upwelling radiation has a relatively high polarization from the horizon to near the Brewster angle (zenith angle of 127°). Just below the ocean surface, the polarization is a maximum near the horizon. The downwelling radiation just below the ocean surface is the only radiation that is strongly elliptically

Digitized by Google
Original from UNIVERSITY OF MICHIGAN
Generated for member (University of Maryland, College Park) on 2014-10-01 20:07 GMT / http://hdl.handle.net/2027/mdp.39015000504624
Public Domain, Google-digitized / http://www.hathitrust.org/access_use#pd-google

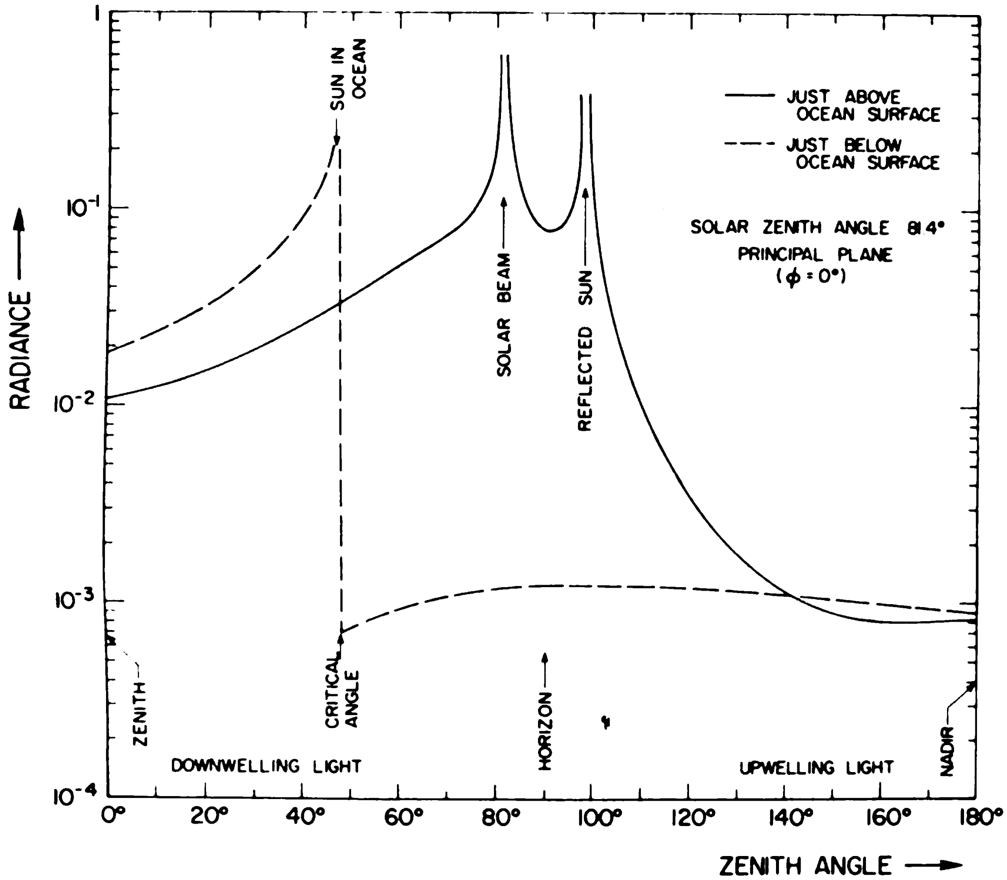

Figure 7 – The radiance in the principal plane just above and just below the ocean surface as a function of the zenith angle of observation when the solar zenith angle is 81.4°.

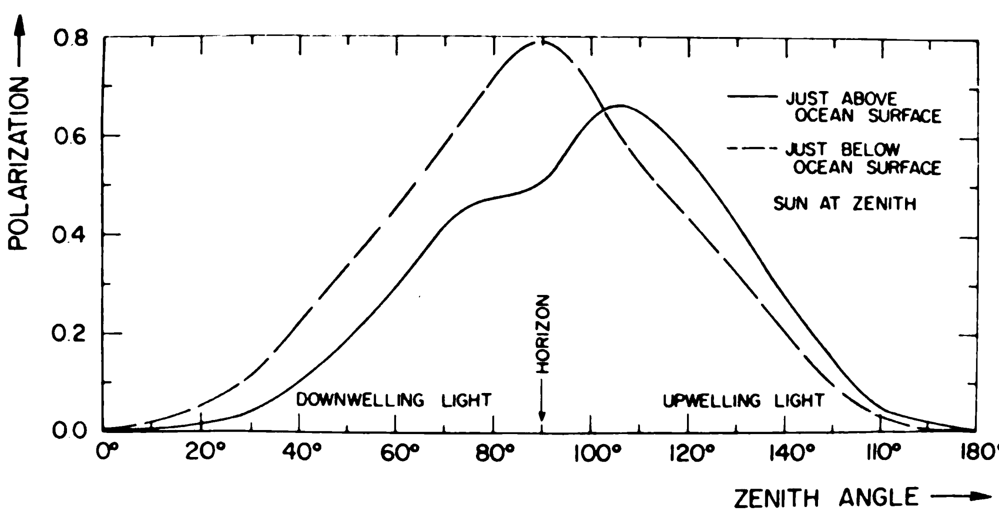

Figure 8 – The polarization of the radiation just above and just below the ocean surface as a function of the zenith angle of observation when the sun is at the zenith.

Generated for member (University of Maryland, College Park) on 2014-10-01 20:07 GMT / http://hdl.handle.net/2027/mdp.39015000504624
Public Domain, Google-digitized / http://www.hathitrust.org/access_use#pd-google
Digitized by Google
Original from UNIVERSITY OF MICHIGAN

polarized. This arises during the process of the total internal reflection of the portion of the upwelling radiation incident at angles greater than the critical angle.

Many marine animals have eyes that detect polarized light. Experiments have shown that some of these animals use polarized light to determine direction, particularly underwater. The polarization is in general a maximum near the horizon and at right angles to the principal plane. Thus it can be used to mark particular directions and orientations under water. There is no evidence that animals can detect elliptically polarized light.

The waves on the ocean surface may appreciably alter the radiance distribution within the ocean as shown in Figure 9. When there is no wind, a flat ocean surface, and the sun is at a zenith angle of 80°, the downwelling radiance increases from the zenith until it reaches a maximum just before the critical angle is reached at 48°. The radiance just below the surface then abruptly decreases by three orders of magnitude as the zenith angle further increases. When there is a 20 knot wind making waves, this radiance distribution is smoothed out by the many different slopes of the wave facets. The maximum in the radiance just below the ocean surface is now at 55° and is much broader than was the case when there were no waves. One has to look at a zenith angle of 75° in order to find a radiance value as low as those found at 50° when the surface is smooth.

It is interesting to remember that the horizon can be seen at sea only because there are waves. If the surface were flat, all the photons traveling downward from the sky at a near grazing angle to the ocean surface would be reflected by the surface (reflectivity approaches unity as zenith angle approaches 90°). Thus the radiance observed at a small angle θ just above the horizon would be the same as that seen by reflection at the same angle θ just below the horizon. This is no longer true when there are waves. First, the photons observed traveling horizontally may have been reflected by a tilted wave facet and thus the angle of reflection is no longer 90°; and appreciable fraction of the photons are then transmitted into the ocean, thus reducing the intensity observed in the horizon direction. Second, the tilted wave facets reflect downwelling photons coming from parts of the sky well above the horizon into the horizontal direction. Since on a reasonably clear day, the sky radiance usually decreases away from the horizon (at least for a certain angular range), there are fewer photons to be reflected to the observer. These two factors combine to decrease the intensity just below the horizon compared to that just above when waves are present.

Digitized by Google
Original from
UNIVERSITY OF MICHIGAN
Generated for member (University of Maryland, College Park) on 2014-10-01 20:07 GMT / http://hdl.handle.net/2027/mdp.39015000504624
Public Domain, Google-digitized / http://www.hathitrust.org/access_use#pd-google

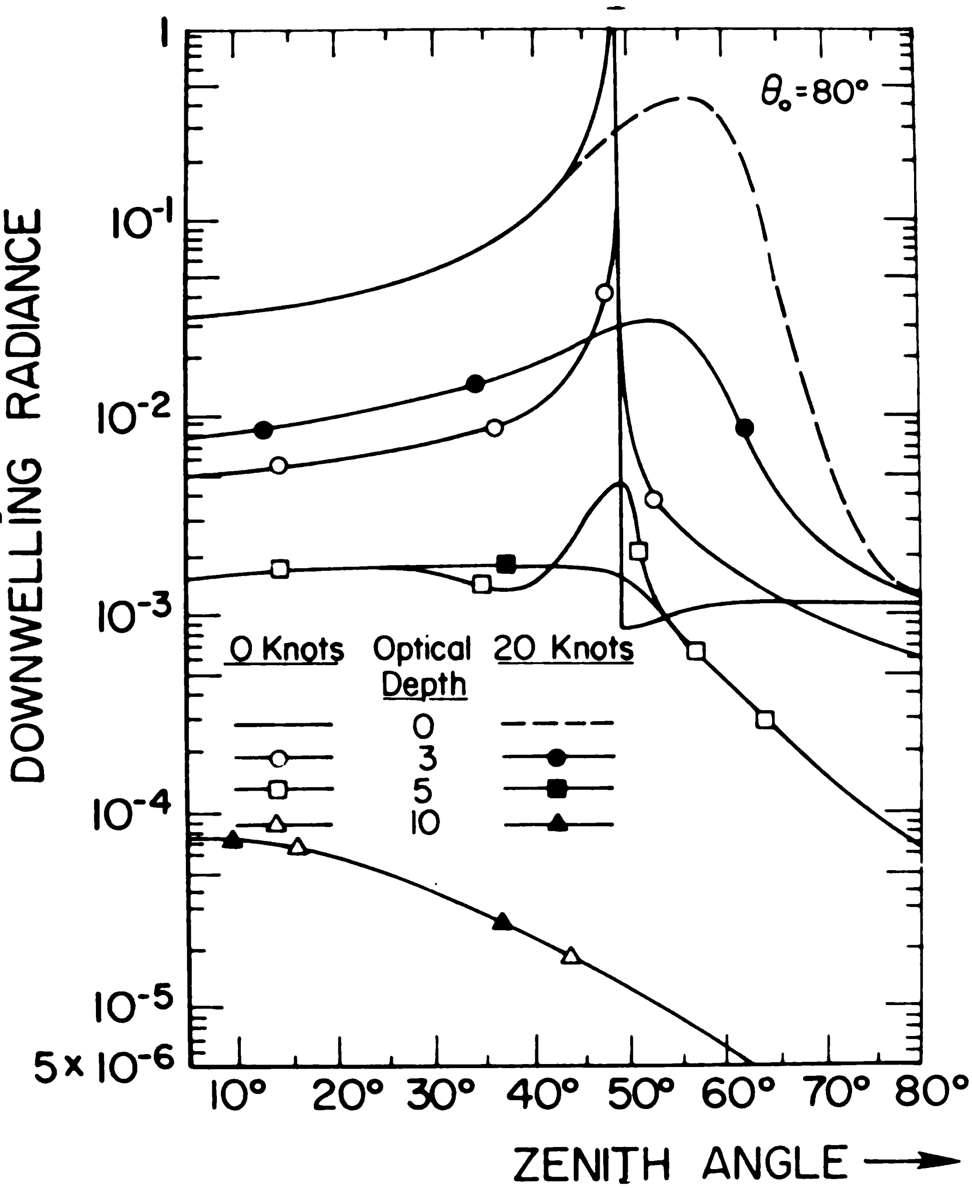

Figure 9 — The downwelling radiance in the ocean at various optical depths (0, 3, 5, 10) beneath the surface. The solar zenith angle is 80°. Curves are shown for both a calm ocean and when there is a 20 knot wind.

Generated for member (University of Maryland, College Park) on 2014-10-01 20:07 GMT / http://hdl.handle.net/2027/mdp.39015000504624
Public Domain, Google-digitized / http://www.hathitrust.org/access_use#pd-google
Digitized by Google
Original from
UNIVERSITY OF MICHIGAN

Photons in the Deep Ocean

As radiation penetrates deep into the ocean, an interesting transformation takes place. An example is shown in Figure 10 where the initial solar zenith angle in the ocean is 31.4°. For simplicity, in this calculation done by the matrix operator technique, only the direct solar beam is incident on the ocean with no sky radiation. At first, near the ocean surface, the maximum radiance is near 31°. As the depth in the ocean increases, the maximum moves toward the zenith. (Figure 10 shows curves for various optical depths defined as the attenuation coefficient times the actual depth. In the blue-green, unit optical depth corresponds to 50 meters in very clear water and 20 meters in moderately clear water.) Finally at great depths the maximum is at the zenith and there is no longer any azimuthal variation of the radiance. This is called the diffusion region, since the photons have undergone so many scattering events by the time that they reach these great depths that they lose all memory of the initial solar direction. In order to see the change in the shape of the radiance better, the nearly exponential decrease in the flux with depth has been taken out of the results in this figure. Thus these

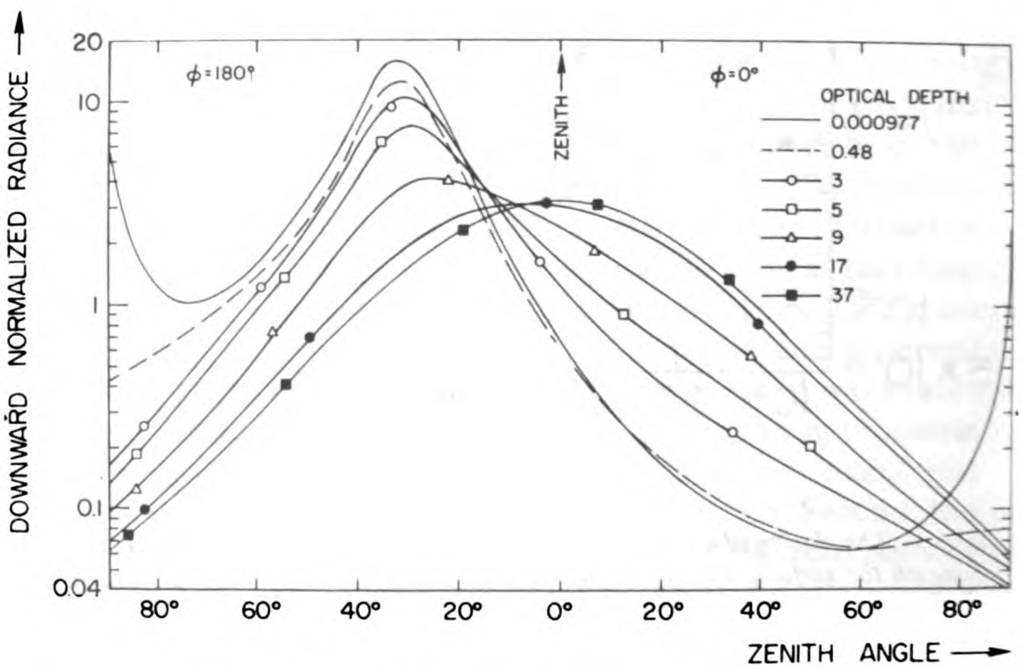

Figure 10 – Downward normalized radiance in ocean as a function of zenith angle of observation for a solar zenith angle in the ocean of 31.4°. Curves are shown at various optical depths within the ocean. The downward normalized radiance is obtained by multiplying the radiance by the factor (π/diffuse downward flux at given optical depth).

Generated for member (University of Maryland, College Park) on 2014-10-01 20:07 GMT / http://hdl.handle.net/2027/mdp.39015000504624
Public Domain, Google-digitized / http://www.hathitrust.org/access_use#pd-google
Digitized by Google
Original from
UNIVERSITY OF MICHIGAN

calculations confirm the often observed fact that, deep in the ocean, there is a strong radiance maximum at the zenith, with a rapid drop-off toward the horizon. Further calculation shows that the upward radiance decreases from the horizon to a minimum value at the nadir.

Color of the Ocean

The color of the ocean depends on a combination of many different factors. First, pure water scatters blue light preferentially and absorbs strongly at the red end of the spectrum. The minimum absorption is around 0.45 microns in the blue region of the spectrum. Thus a deep body of nearly pure water appears blue when seen from above in reflected sunlight. Similarly deep in the water, all wavelengths are absorbed except those near the absorption minimum, so that the light is also blue at great depths. In the real ocean there are also varying amounts of various inorganic and organic substances. The hydrosols of interest here include all types of particles whose size is such that they can appreciably interact with the light. The amount present varies through a large range from pure waters to muddy coastal waters.

The hydrosols have two effects on the light. First, they scatter the light predominantly in the forward direction, since many of these particles are somewhat larger than the wavelength of visible light. Second, as the hydrosol amount increases, the minimum absorption of the water moves to the blue-green and then to the green region of the spectrum.

In addition, both chlorophyll and yellow substance absorb light. Chlorophyll has an important absorption band around 0.44 micrometers. Water that has a typical chlorophyll amount has an absorption maximum at 0.44 micrometers, while the absorption minimum is shifted to 0.51 micrometers. This minimum occurs at ever higher wavelengths as the chlorophyll amount further increases.

The amount of chlorophyll in ocean water can be judged approximately from the observed color on a clear day. A deep blue ocean has relatively little chlorophyll; as the color changes to greenish-blue and to green there are larger and larger amounts in general.

The color observed deep in the ocean corresponds closely to the wavelength of minimum absorption. Thus this color also changes to greenish-blue and green as the hydrosol and chlorophyll amounts increase.

Digitized by Google
Original from UNIVERSITY OF MICHIGAN
Generated for member (University of Maryland, College Park) on 2014-10-01 20:07 GMT / http://hdl.handle.net/2027/mdp.39015000504624
Public Domain, Google-digitized / http://www.hathitrust.org/access_use#pd-google

The color of the ocean as observed from above also depends on atmospheric conditions as well as the chlorophyll amount. When the sky is clear and deep blue, this light is reflected at the ocean surface and adds to the observed blue color of the ocean. The grey sky of an overcast day mutes the color of the ocean.

Exactly how changes in all of these quantities influence the color of the ocean is being studied by the Monte Carlo method with our ocean models.

When the ocean surface is observed at a particular angle, the observed light comes from three different sources: (1) the direct solar beam reflected by the surface (forming the glitter pattern; (2) the sky radiation also reflected by the surface; (3) upwelling light from within the ocean that is refracted through the surface. There has been little evidence in the past as to the relative contribution of these three factors under various conditions. Our calculations show when each factor is dominant for a particular set of conditions. The results for a clear day and a relatively clear ocean are shown in Figs. 11 and 12. The results are shown for four solar zenith angles, 15°, 32°, 57°, and 80°. Only a half plane is shown for each solar zenith angle, since the curves are symmetric across the principal plane. These are polar plots with the nadir at the center and the horizon at the edge. A wind speed of 20 knots and a corresponding wave slope distribution is assumed.

The reflected sky radiation is always dominant over a strip of the sky from the horizon up to some angle determined by the solar zenith angle. The higher reflectivity of the surface for photons incident to the surface at a near grazing angle always makes this the dominant component of the radiation near the horizon. As the angle of observation increases from the horizon, the upwelling radiation from the ocean begins to dominate at some point. Finally the glitter pattern of the reflected solar beam dominates over some range of angles determined again by the solar zenith angle.

A theoretical study of the distribution of light in the ocean can provide valuable insight into the importance of the many different factors that influence it. The reasonableness of the models is determined by comparison with experimental measurements. It is not possible to vary the chlorophyll amount, the amount of yellow substance, the wave slopes, the amount and character of the hydrosols, and the atmospheric conditions and cloud amount in the real ocean in a controlled way. With numerical experiments each of these factors can be changed in turn and their influence and importance determined.

Digitized by Google
Original from
UNIVERSITY OF MICHIGAN
Generated for member (University of Maryland, College Park) on 2014-10-01 20:07 GMT / http://hdl.handle.net/2027/mdp.39015000504624
Public Domain, Google-digitized / http://www.hathitrust.org/access_use#pd-google

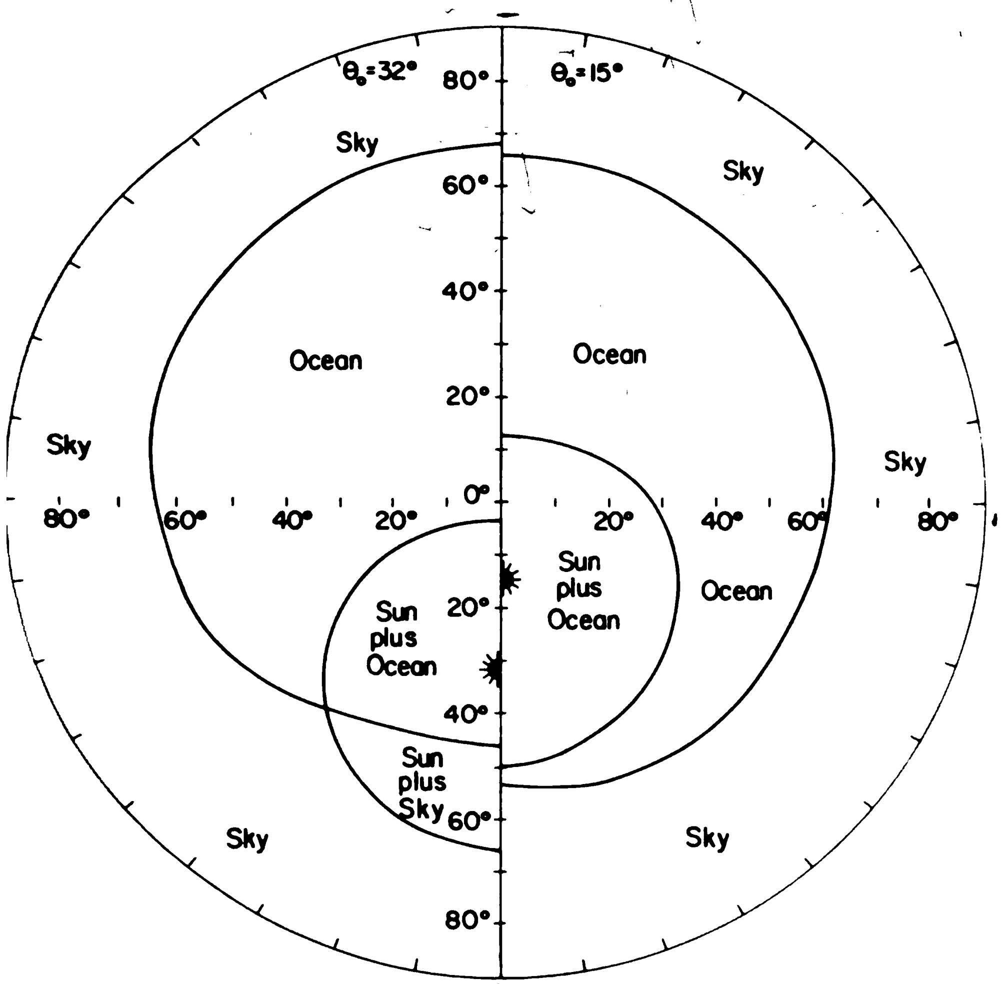

Figure 11 — Polar plot showing type of upwelling radiation that dominates when viewing the ocean surface at a given angle. The right half of the diagram is for a solar zenith angle of 15°, while the left half is for 32°. The principal plane corresponds to the vertical line in the center of diagram, while the outermost circle is the horizon. The reflected sky radiation always dominates the observed radiation near the horizon. When looking nearer the nadir, the upwelling radiation that comes from within the ocean dominates. Near the mirror angle for the solar radiation, the glitter pattern of the sun dominates with a background of radiation from one of the two sources mentioned above. A wind speed of 20 knots is assumed to calculate the glitter pattern.

Digitized by Google
Original from UNIVERSITY OF MICHIGAN
Generated for member (University of Maryland, College Park) on 2014-10-01 20:07 GMT / http://hdl.handle.net/2027/mdp.39015000504624
Public Domain, Google-digitized / http://www.hathitrust.org/access_use#pd-google

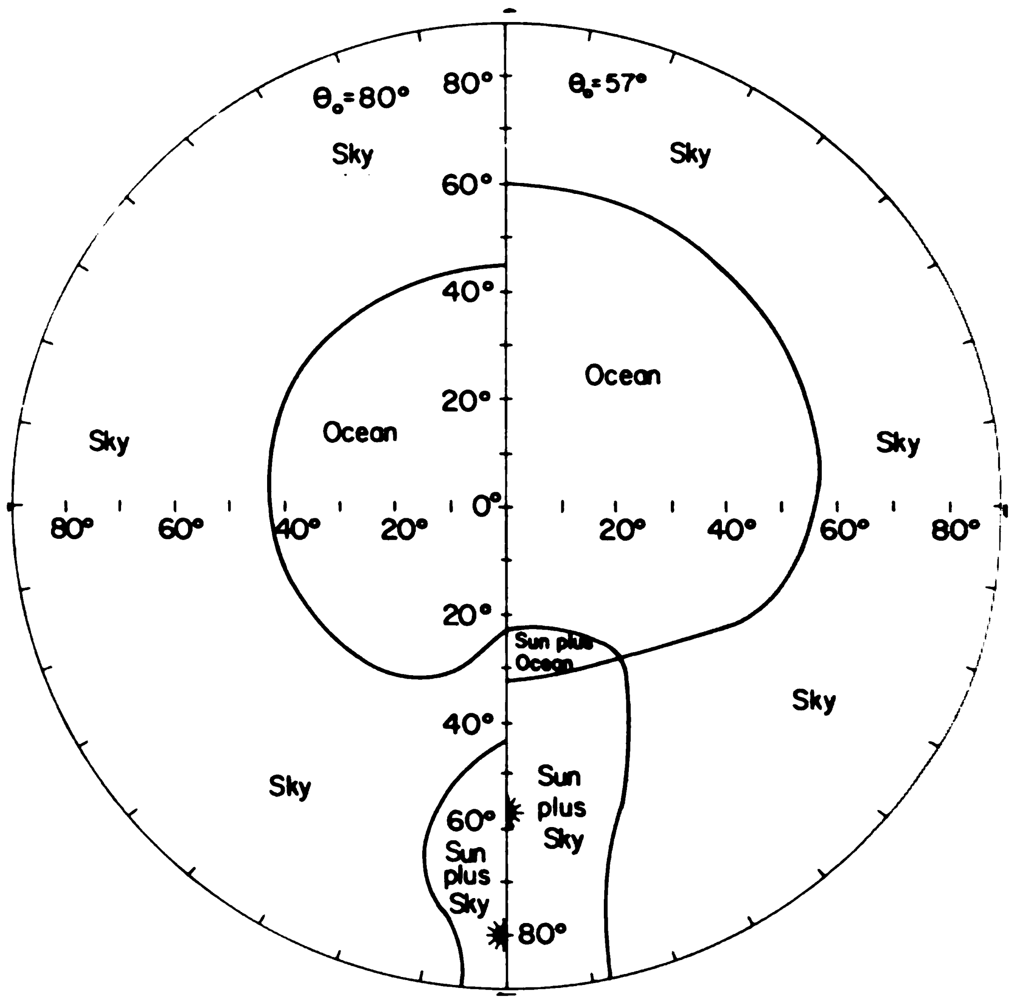

Figure 12 — Same as Figure 11 except solar zenith angles are 57° and 90°.

References

1. N. G., Jerlov, Optical Oceanography (Elsevier Publishing, New York, 1968), 194 pp.
2. N. G. Jerlov and E. S. Nielsen, Editors, Optical Aspects of Oceanography, (Academic Press, New York, 1974), 494 pp.
3. G. W. Kattawar, G. N. Plass, and J. A. Guinn, Jr., "Monte Carlo Calculations of the Polarization of Radiation in the Earth's Atmosphere-Ocean System," *J. Phys. Oceanog.* 3, 353-372, 1973.
4. G. W. Kattawar and G. N. Plass, "Interior Radiance in Optically Deep Absorbing Media," *J. Quant. Spectrosc. Radiat.* Transfer, 13, 1065-1080 (1973); 13, 1081-1096 (1973); 15, 61-85 (1975).
5. G. N. Plass and G. W. Kattawar, "Monte Carlo Calculations of Radiative Transfer in the Earth's Atmosphere-Ocean System," *J. Phys. Oceanog.* 2, 139-145 (1972); 2, 146-156 (1972).
6. G. N. Plass, G. W. Kattawar, and J. A. Guinn, Jr., "Radiative Transfer in the Earth's Atmosphere and Ocean: Influence of Ocean Waves," *Appl. Opt.* 14, 1924-1936 (1975).

Generated for member (University of Maryland, College Park) on 2014-10-01 20:07 GMT / http://hdl.handle.net/2027/mdp.39015000504624
Public Domain, Google-digitized / http://www.hathitrust.org/access_use#pd-google
Digitized by Google
Original from
UNIVERSITY OF MICHIGAN

Spin Entry of Aircraft

S. B. Spangler*
Nielsen Engineering and Research, Inc.

Introduction

With the increasingly severe requirements on high speed performance and maneuverability, fighter-bomber aircraft have become much more prone to reaching flight conditions from which spins can readily develop. For performance reasons, this class of aircraft tends to have slender pointed noses and highly swept, low aspect ratio wings with leading edge extensions, or strakes. A good example is the F-5, shown in three-view in Figure 1.

There are many conflicting restraints on the design of such an aircraft. It has only been in the last several years, however, that high angle of attack and spin departure characteristics have been recognized as factors of major importance in the initial design. Although the problem has been recognized, the actual understanding of the flow phenomena has been very slow in coming.

Several years ago, NASA began a fundamental program directed towards understanding the behavior of these types of aircraft at spin departure, in a fully developed spin, and during spin recovery. The aircraft manufacturers, of course, of course, are vitally interested in these areas, although their efforts are less well known because of proprietary aspects of aircraft design competition. The military is vitally interested, because of the considerable loss in equipment, and in some cases lives, due to spin-related accidents. All of these factors have contributed to considerable activity in spin-related aerodynamics and high angle of attack aircraft behavior.

Most of the work has been experimental in nature. Examples include the systematic wind tunnel work that the NASA Langley Research Center did on the F-5 configuration (1) and the F-4 configuration (2-4), and work to examine modifications to aircraft configurations to improve high angle of attack directional aerodynamic characteristics (5 and 6). However, relatively little work has been done to understand the basic flow characteristics and force distributions acting on an aircraft at incipient spin entry. Two years

*Mr. Spangler is Vice President of Neilsen Engineering and Research Inc., Mountain View, California. His field of interest is low speed aerodynamics.

Digitized by Google
Original from UNIVERSITY OF MICHIGAN
Generated for member (University of Maryland, College Park) on 2014-10-01 20:07 GMT / http://hdl.handle.net/2027/mdp.39015000504624
Public Domain, Google-digitized / http://www.hathitrust.org/access_use#pd-google

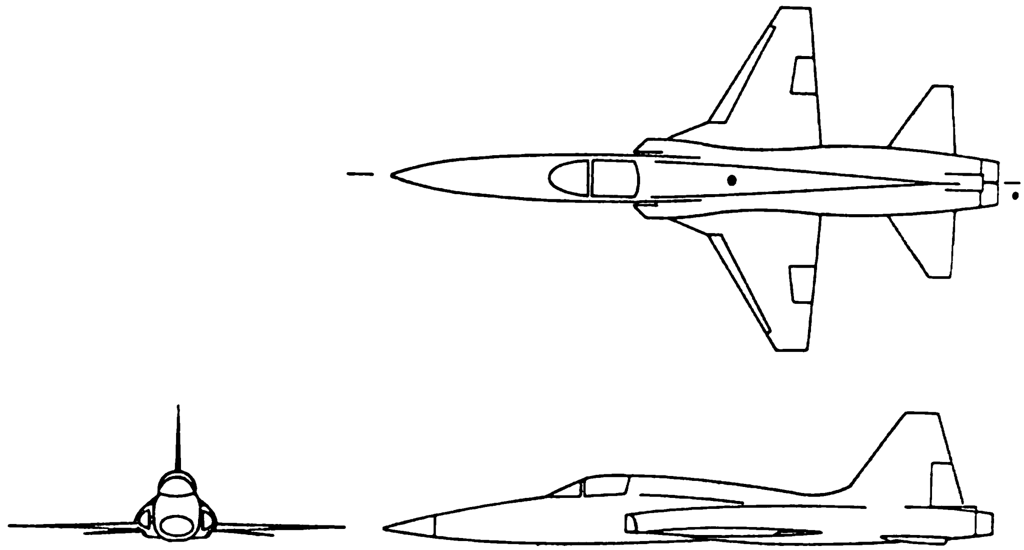

Figure 1 — Three-view Sketch of F-5 Aircraft

ago, the Office of Naval Research began a project at Nielsen Engineering & Research, Inc. directed towards this end.

Nature of the Problem

The flight condition at incipient spin entry for high speed fighter aircraft is a high angle of attack (25° to 50°), a small (or zero) angle of sideslip (less than 10° or 15°) and a moderate subsonic speed. Under these conditions, the wing and horizontal tail are well stalled with flow separation occurring along the leading and side edges. If a highly swept strake is present, its separated flow is probably organized as a vortex lying above and inboard of the leading edge.

The flow over the nose is also separated and plays the key role in development of the yawing moments that cause departure motions such as "nose slice." It has long been recognized that the separated flow over long slender bodies of revolution becomes asymmetric as the angle of attack is raised above about 25°. When fighter aircraft, in particular the F-4 and F-111, began to use long pointed noses for low supersonic drag, undesirable spin departure characteristics were noted; and the cause was laid to asymmetric separation on the nose (7).

The separated flow takes the form of vortex sheets which emanate at the separation lines along the sides of the nose and roll up over the nose to form regions of concentrated vorticity, much as shown below. These cause a side force on the nose which is well ahead of the aircraft center of gravity and produces a large yawing moment at

Digitized by Google
Original from
UNIVERSITY OF MICHIGAN
Generated for member (University of Maryland, College Park) on 2014-10-01 20:07 GMT / http://hdl.handle.net/2027/mdp.39015000504624
Public Domain, Google-digitized / http://www.hathitrust.org/access_use#pd-google

zero sideslip. What could be equally significant is that these vortices pass aft over the wing and tail and cause side force distributions on these components as well, which may augment or diminish the nose-induced yawing moment. The asymmetry may develop either to the right or left, depending on small asymmetries in the nose shape, and sideslip will either augment or diminish the yawing moments. Additionally, the damping in yaw, which may either propel the aircraft to higher angular rates or damp the angular motion, is dominated by the vortex behavior (Figure 2).

Finally, it is clear that the nose shape itself has a great influence on the development of the vortex system. The F-5, for example, shows high side force and yawing moment at zero sideslip and high angles of attack ($>30^\circ$), but the nose alone shows very little side force, unlike a circular cross-sectional nose. As a result, the complete configuration shows quite different behavior, particularly at small sideslip, than does the F-4, for example, at high angles of attack.

Figure 3 shows the typical yawing moment derivative (Cn_β) over a range of angle of attack for the two aircraft. At low angles, both aircraft show a conventional positive (stable) directional stability. At angles above 22°, the F-4 derivative becomes negative, whereas the F-5 derivative remains positive. The F-5 nose-alone curve is shown to illustrate a conventional destabilizing influence at small angles but a stabilizing influence at high angles with values very close to those of the complete configuration.

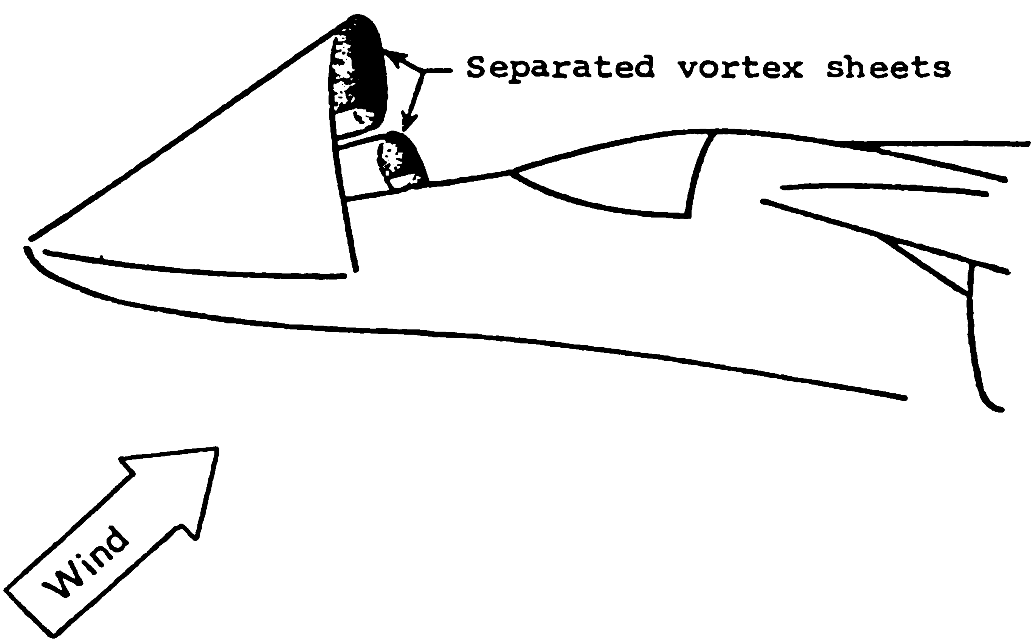

Figure 2 — Asymmetric Vortex Separation on An Aircraft Nose

Digitized by Google
Original from
UNIVERSITY OF MICHIGAN
Generated for member (University of Maryland, College Park) on 2014-10-01 20:07 GMT / http://hdl.handle.net/2027/mdp.39015000504624
Public Domain, Google-digitized / http://www.hathitrust.org/access_use#pd-google

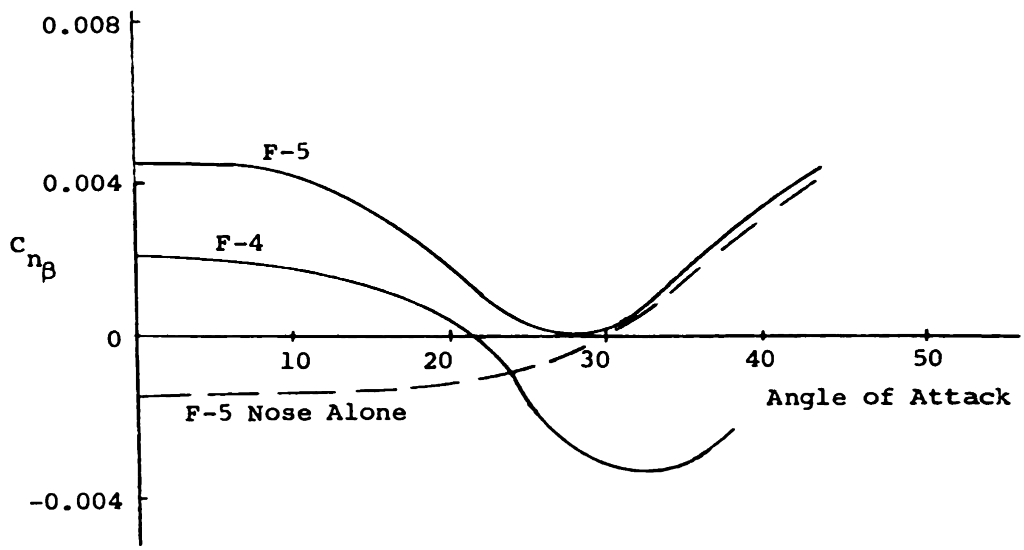

Figure 3 — Variation of Yawing Moment Derivative with Angle of Attack for F-4 and F-5 Configurations

Analytical Model

In order to investigate the distribution of lateral forces on an aircraft at high angles of attack, an analytical model was developed to predict the nonlinear side force effects. The general approach is to characterize the separation vortical flow off the nose as potential vortices which then stream aft over the wing, body, and tail. Classical potential flow wing-body-tail interference methods (8) can then be used to calculate the nonlinear interference effects. The resulting model is then the one shown in Figure 4.

The nose may shed two or perhaps three vortices, the strakes will shed separation vortices, and the wing load distribution and wake can be described in terms of a trailing vortex wake. These vortices all interact to modify the positions of each other, and all induce loads on all aircraft components aft of the positions at which they are formed. The problem consists of defining the positions and strengths of these vortices, in the presence of the flow field induced by each other and the free-stream flow over the wing, body, and tail, and then calculating the loads induced on the components by the vortices.

Figure 4 shows four regions of the aircraft, each of which are treated separately: nose, wing-body, afterbody, and tail. The detailed description of the flow models used and/or developed is given in reference 9. A summary description is given here to indicate the general approach.

Digitized by Google
Original from
UNIVERSITY OF MICHIGAN
Generated for member (University of Maryland, College Park) on 2014-10-01 20:07 GMT / http://hdl.handle.net/2027/mdp.39015000504624
Public Domain, Google-digitized / http://www.hathitrust.org/access_use#pd-google

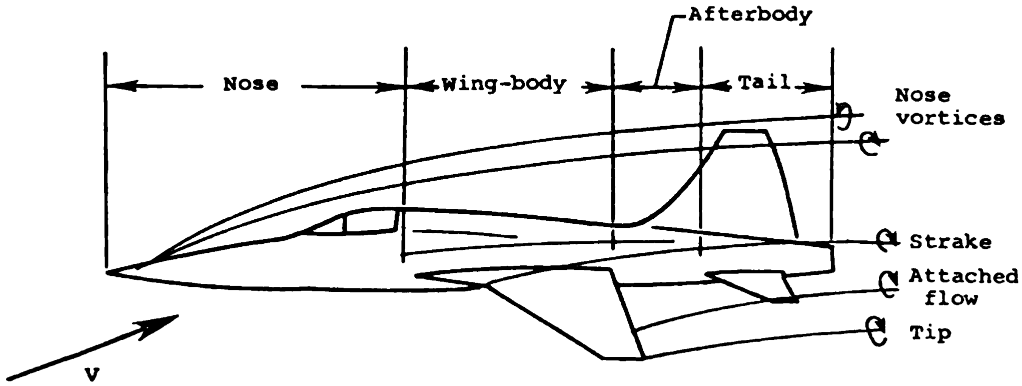

Figure 4 — Vortex Interference on Various Aircraft Components

Nose

The two principal methods that have been developed to describe asymmetric vortex shedding are those of Thomson (10) and Wardlaw (11). Both are limited to bodies of circular cross section.

The Thomson model is based primarily on extensive experimental data on long cone-cylinders in which many vortices are formed and "torn" from the feeding sheet at the separation line to move aft at a direction close to the free-stream direction. If one looks at the flow in a plane normal to the body axis near the base, the vortex positions in this plane resemble the von Kármán vortex streak downstream of a cylinder in two-dimensional flow. The position and strength of each of these vortices is regular except for the first two, which are influenced by the conical forebody. Thus, the method is applicable primarily to missile-type configurations with long cylindrical afterbodies, and does not yield good information on the positions and strengths of the first two or three vortices formed on the nose or the load distribution induced on the nose.

Wardlaw's method is based on a slender-body analysis in which the steady three-dimensional flow can be analyzed as an unsteady, two-dimensional flow in a plane normal to the body axis, with time in the two-dimensional problem equivalent to distance along the body in the three-dimensional problem. He supposes two small vortices to be inserted in the flow near the separation lines at zero time (the nose tip), which move away and become increasingly asymmetric with time. If the nose is sufficiently long, the vortex furtherest from the body will be "torn" from the body according to an empirical criterion, and a third one is then formed at the separation point on that side. This method gives great detail on the positions, strengths, and induced loads along the nose, but requires

Digitized by Google
Original from UNIVERSITY OF MICHIGAN
Generated for member (University of Maryland, College Park) on 2014-10-01 20:07 GMT / http://hdl.handle.net/2027/mdp.39015000504624
Public Domain, Google-digitized / http://www.hathitrust.org/access_use#pd-google

input of the separation line locations on the body and several empirical parameters. The accuracy of the method is impossible to determine because of the lack of flow field measurements on noses.

Wing-Body

The method of calculating wing-body characteristics in the presence of the nose vortices consists of a vortex-lattice lifting-surface program in which an arbitrary asymmetric velocity distribution can be specified over the wing surface. The body is assumed circular in cross section and is combined with the wing by the use of image vortices within the body. Flow separation at the leading edge is treated through the vortex-lift concept of Polhamus (12), which assumes that leading edge suction (calculated from the vortex-lattice method) is rotated into the lift direction by leading edge separation. With an asymmetric velocity distribution such as would be induced by the nose vortices passing over the wing, a side force, yawing moment and rolling moment will be predicted by the method.

As a part of this computer program, a slender-body method is used to compute the path of the nose vortices as they pass over the wing-body. This method uses two-dimensional techniques to map the wing-body into a circle and compute the velocities at each vortex in the plane normal to the body axis to define the vortex positions at a series of normal planes along the wing chord. Once these vortex positions are known, induced velocities on the wing are calculated.

Afterbody

The afterbody is assumed circular, and slender-body methods similar to those discussed above for the wing-body are used to calculate the vortex positions along the afterbody. Since the afterbody is aft of the wing trailing edge, the wake vortices from the wing must be included with the nose vortices. For this purpose, the wing panel lift is considered to be represented by a leading edge separation vortex and an attached flow vortex, with strengths associated with the amount of lift and the position (span) of the vortex.

The forces induced on the afterbody by the vortices can be calculated from the vortex strengths and positions at the forward and aft stations of the afterbody using vortex-impulse relations.

Digitized by Google
Original from
UNIVERSITY OF MICHIGAN
Generated for member (University of Maryland, College Park) on 2014-10-01 20:07 GMT / http://hdl.handle.net/2027/mdp.39015000504624
Public Domain, Google-digitized / http://www.hathitrust.org/access_use#pd-google

Tail

The tail loads are calculated knowing the vortex strengths and positions at the tail leading edge (from the afterbody calculations) using strip theory methods (13).

Results

In order to get some insight into the distribution of lateral loads on a fighter at high angles of attack, some calculations were made for the F-5 configuration and compared with data from the investigation of reference 1. Since the available methods for nose vortex shedding cannot take account of noncircular nose characteristics, which for the F-5 are significantly different than a typical circular body, the data comparisons are of interest principally from a qualitative standpoint.

The predicted division of loads in coefficient form between the four regions of the aircraft, together with measured overall quantities (no breakdown is available) are the following for 40° angle of attack and zero sideslip:

	Side Force	Yawing Moment	Rolling Moment
Nose	+0.103	+0.0751	0
Wing-Body	+0.0968	+0.0003	-0.022
Afterbody	+0.106	-0.0301	0
Tail	+0.0594	-0.0242	-0.0277
Sum	+0.3652	+0.0211	-0.0497
Measured	+0.062	+0.0215	-0.009

Considering first the predicted values, one notes that all four regions of the configuration contribute substantially equally to the side force. Because of the moment arms, the yawing-moment contributions are of varying size, with the nose being the major contributor. Only the wing and tail contribute to the rolling moment and in approximately equal amounts. The general observation of interest is that the nose is not the only substantial contributor to lateral effects, but the nose asymmetric vortex influence extends to all components of the aircraft.

Digitized by Google
Original from
UNIVERSITY OF MICHIGAN
Generated for member (University of Maryland, College Park) on 2014-10-01 20:07 GMT / http://hdl.handle.net/2027/mdp.39015000504624
Public Domain, Google-digitized / http://www.hathitrust.org/access_use#pd-google

The comparison of measured and predicted values indicates similar signs for the forces and moments but considerably higher predicted than measured values. The good agreement on yawing-moment coefficient is probably fortuitous, since the sum is the difference between numbers large with respect to it. Since the source of all these effects is the nose vortices, which were calculated based on circular nose characteristics, the differences between predicted and measured values are not entirely unexpected.

The conclusion that all components of the aircraft contribute substantially to the yawing moments at high angles of attack is also borne out by the data in the experiments of reference 1, which show substantial yawing moment on the complete aircraft and essentially no moment on the nose alone at high angle of attack and zero sideslip. Thus, the positions and strengths of the nose vortices are most important in determining the loads on the aircraft at spin entry.

What's Ahead

In order to really understand the origin of the lateral effects on a pointed-nose aircraft at incipient spin entry, it is necessary to define the separated flow field above the nose and the interaction of the resulting vortex system with the wing, body, and tail. At the present time, no satisfactory measurements exist on real aircraft noses or on the interaction of asymmetric nose vortices with downstream components. Two test programs are planned to supply this kind of information.

The first program will involve tests on aircraft nose shapes in the Nielsen Engineering water tunnel. Models will be tested on strain gage balances to measure the forces and moments and, at the same time, flow visualization techniques will be used to try to identify the number and position of the separation vortices. Test models will include simply cross-sectional shapes, such as an ellipse, and a real aircraft shape (the F-5 nose). These results should provide considerable insight into the nature of the flow and origin of forces and methods of analytically modeling the flow on noses of aircraft.

The second program is a cooperative test program between the Office of Naval Research and the NASA Langley Research Center, in which tests are to be conducted on a research V/STOL configuration to simultaneously measure forces and moments on the complete configuration and flow field velocity measurements over the model. The flow field measurements will be taken at two axial stations: one just ahead of the wing and one at the wing trailing edge. The results

Generated for member (University of Maryland, College Park) on 2014-10-01 20:07 GMT / http://hdl.handle.net/2027/mdp.39015000504624
Public Domain, Google-digitized / http://www.hathitrust.org/access_use#pd-google
Digitized by Google
Original from
UNIVERSITY OF MICHIGAN

of these tests will provide information on formation of the nose vortices and their interaction with the wing and strake vortices.

Out of this work should come greater insight into the characteristics which can be employed in the design of fighter-bomber aircraft to provide more favorable high angle of attack aerodynamic behavior and greater resistance to spin.

References

1. S. B. Grafton, J. R. Chamber, and P. L. Coe, Wind-Tunnel Free-Flight Investigation of a Model of a Spin-Resistant Fighter Configuration. NASA TN D-7716, June 1974.
2. E. L. Anglin, Static Force Tests of a Model of a Twinjet Fighter Airplane for Angles of Attack from -10° to 110° and Sideslip Angles from -40° to 40°. NASA TN D-6425, Aug. 1971.
3. S. B. Grafton and Libbey, Dynamic Stability Derivatives of a Twinjet Fighter Model for Angles of Attack from -10° to 110°. NASA TN D-6091, Jan. 1971.
4. P. L. Coe and W. A. Newsom, Wind Tunnel Investigation to Determine the Low-Speed Yawing Stability Derivatives of a Twin-jet Fighter Model at High Angles of Attack. NASA TN D-7721, Aug. 1974.
5. W. R. Burris, Effect of Wing Leading Edge Geometry on Maneuvering Boundaries and Stall Departure. AIAA Paper No. 70-904, 1970.
6. E. J. Ray and E. G. Hollingsworth, Subsonic Characteristics of a Twin-jet Swept-Wing Fighter Model with Maneuvering Devices. NASA TN D-6921, Jan. 1973.
7. J. R. Chambers, E. L. Anglin, and J. S. Bowman, Effects of a Pointed Nose on Spin Characteristics of a Fighter Airplane Model Including Correlation with Theoretical Calculations. NASA TN D-5921, Sept. 1970.
8. J. N. Nielsen, *Missile Aerodynamics*. McGraw-Hill Book Company, Inc., New York, 1960.
9. S. B. Spangler and J. N. Nielsen, Exploratory Study of Aerodynamic Loads on a Fighter-Bomber at Spin Entry. Nielsen Engineering & Research, Inc. TR 87, May 1975.
10. K. D. Thomson, The Estimation of Viscous Normal Force, Pitching Moment, Side Force, and Yawing Moment on Bodies of Revolution at Incidence up to 90°. Dept. of Supply, Australian Defense Scientific Service, Weapon Research Establishment, Salisbury, Australia, WRE Report 782, Oct. 1972.
11. A. B. Wardlaw, Prediction of Normal Force, Pitching Moment, and Yawing Force on Bodies of Revolution at Angles of Attack up to 50 Degrees Using a Concentrated Vortex Flow-Field Model. NOL TR 73-209, Oct. 1973.
12. E. C. Polhamus, "Predictions of Vortex Lift Characteristics by a Leading Edge Suction Analogy," *Jour. of Aircraft*, vol. 8, no. 4, Apr. 1971.
13. W. C. Pitts, J. N. Nielsen, and G. E. Kaattari, Lift and Center of Pressure of Wing-Body-Tail Combinations at Subsonic, Transonic, and Supersonic Speeds. NACA Rept. 1307, 1975.

Generated for member (University of Maryland, College Park) on 2014-10-01 20:07 GMT / http://hdl.handle.net/2027/mdp.39015000504624
Public Domain, Google-digitized / http://www.hathitrust.org/access_use#pd-google
Digitized by Google
Original from
UNIVERSITY OF MICHIGAN

Research Notes

A Possible Fracture Zone in the Fiji Plateau

Among the most intriguing sea-floor structures to be recognized from the concept of plate tectonics are fracture zones, or transform faults. These structural features of crustal plates make up the boundaries along which there is horizontal motion, one plate to the next. This motion is distinct from collision boundaries (where two plates meet head on) or spreading, or trailing boundaries.

That there is horizontal movement is not in itself of great moment, but that transform faults end at either spreading centers, subduction zones, or both, thereby becoming transformed from a fault to another structure, is a totally new concept of crustal motion. Furthermore, the action along transform faults (fracture zones) is at spreading center and subduction zones. In between they become, in effect, "fossil faults." Consequently, when seismic activity in the ocean's crust is strong where topography indicates a fracture zone, a spreading center is probably in the area as well.

Although the ocean's crust around it had been studied, the Fiji Plateau was not as well known before John Halunen, graduate student at the University of Hawaii, made it the subject of his dissertation. During the course of his survey, Mr. Halunen learned that (1) sediments are absent or very thin on the Plateau, (2) heat flow from the oceanic crust is two to four times the average, and (3) the topography clearly indicates a linear topographic feature extending east-west for about 250 miles near latitude 14°S.

This linear feature is probably, Mr. Halunen states, the Hazel Holme Fracture Zone, the existence of which has been questioned recently by some geophysicists. As further favorable evidence, he points to the magnetic anomaly lineations associated with the fracture and the offset to the west of Espiritu Santo Island. If this latter evidence does indicate a right lateral strike slip fault, then two more fracture zones might be present to the south of Espiritu Santo and south of Malekula Island, both of which lie on the east edge of the New Hebrides Ridge.

If these features are indeed fracture zones and if there is a spreading center on the east of the Fiji Plateau, then there should be more seismic activity there than in other parts. This is just what was learned when Japanese ocean bottom seismometers were deployed in 1973. During a 10-day period, an average of 11 micro-earthquakes per day was recorded. The arrival times indicated that the earthquakes were centered near the seismometers on the east side of the Plateau. Several earthquake swarms suggest spreading-center/transform fault activity. On the negative side, however, Halunen's analysis of the magnetic anomalies does not provide a convincing spreading picture.

The Fiji Plateau clearly fits into the Pacific pattern of plates, but there must be much more work than has yet been accomplished to know its actual alignment in Pacific-plate motion.

U. S. GOVERNMENT PRINTING OFFICE : 1976 O - 217-363

Digitized by Google
Original from
UNIVERSITY OF MICHIGAN
Generated for member (University of Maryland, College Park) on 2014-10-01 20:07 GMT / http://hdl.handle.net/2027/mdp.39015000504624
Public Domain, Google-digitized / http://www.hathitrust.org/access_use#pd-google

IN THIS ISSUE

VOL. XXIX, NO. 8

Cover Caption

Shown here is the high performance F14 which has benefited from research in spin entry.

DEPARTMENT OF THE NAVY
OFFICE OF NAVAL RESEARCH
ARLINGTON, VA. 22217

OFFICIAL BUSINESS

PENALTY FOR PRIVATE USE, $300.

POSTAGE AND FEES PAID
DEPARTMENT OF THE NAVY
DoD-316

U.S.MAIL

CONTROLLED CIRCULATION RATE

Generated for member (University of Maryland, College Park) on 2014-10-01 20:07 GMT / http://hdl.handle.net/2027/mdp.39015000504624
Public Domain, Google-digitized / http://www.hathitrust.org/access_use#pd-google

Digitized by Google

Original from
UNIVERSITY OF MICHIGAN